International Journal of Innovative Computing, Information and Control
Volume **21**, Number **3**, June **2025**

ICIC International ©2025 ISSN 1349-4198
pp. **667–682**

MPGA-NET: A MULTI-PATH GUIDED ATTENTION NETWORK FOR DESERT SEISMIC NOISE ATTENUATION

Tie Zhong[1,2] and Yaling Song[2,*]

[1]Key Laboratory of Modern Power System Simulation and Control
and Renewable Energy Technology, Ministry of Education
[2]School of Electrical Engineering
Northeast Electric Power University
No. 169, Changchun Road, Jilin 132012, P. R. China
zht@neepu.edu.cn; *Corresponding author: 2202200365@neepu.edu.cn

Received October 2024; revised February 2025

Abstract. *Desert seismic exploration is a key technology for detecting natural resources. However, due to the unique surface conditions and complex environmental factors in desert regions, seismic data are often contaminated by strong noise, which poses serious challenges for subsequent data processing. Furthermore, background noise not only exhibits high intensity and a wide frequency band but also overlaps with effective seismic signal in the frequency spectrum, rendering it challenging for traditional signal processing techniques to separate noise from signals. In recent years, denoising models based on convolutional neural network (CNN) have shown significant potential for denoising tasks due to their strong feature extraction and learning capabilities. However, existing models have limitations in feature extraction and representation, which may affect denoising performance. To address this shortcoming, this paper proposes a new Multi-Path Guided Attention Network (MPGA-Net). Specifically, MPGA-Net integrates three paths: the primary core path is responsible for multi-scale feature extraction; the guided enhancement path enhances feature representation; and the attention assisted path focuses on key information. Experimental results show that MPGA-Net not only effectively suppresses noise but also recovers weak reflected signals masked by noise, achieving denoising performance that is significantly superior to both traditional methods and existing CNN approaches.*

Keywords: Attention mechanisms, Convolutional neural network (CNN), Desert noise attenuation, MPGA-Net

1. **Introduction.** Seismic exploration is a key method for oil and gas exploration [1]. It involves the deployment of sensors to acquire artificially generated seismic wave signals, which are subsequently processed and analyzed to reveal subsurface geological structures and identify potential mineral resources [2,3]. In recent years, with the ongoing exploitation of natural resources, exploration activities have gradually shifted toward resource-rich desert regions [4]. However, the unique environmental conditions and complex geological structures in these areas have introduced significant challenges to seismic data acquisition. Consequently, compared with traditional exploration regions, seismic records in desert areas are more susceptible to noise interference, such as random noise and surface wave, which significantly degrade the quality and reliability of the data [5,6]. Among these, random noise is primarily caused by environmental factors, such as surface wind, sand movement, and thermal expansion, which manifests as irregular fluctuations and lacks correlation in both time and space [7]. This type of noise easily contaminates reflected signals, greatly reducing the signal-to-noise ratio (SNR) [8]. Meanwhile, surface

DOI: 10.24507/ijicic.21.03.667

wave generated by the interaction of seismic source energy with surface and shallow geological structures is powerful and easily obscures the effective signals, further blurring their characteristics [9,10]. In addition, the energy of reflection signals is typically weaker, and characterized by lower frequencies, generally ranging from 10 to 25 Hz [11]. The frequencies of random noise and surface waves predominantly reside within the 0-20 Hz range, leading to an overlap between the signal and noise spectra, thereby exacerbating the challenges associated with noise suppression [12,13]. Therefore, the effective suppression of noise interference and the recovery of critical seismic signals during desert seismic exploration have become urgent technical challenges that need to be addressed.

For an extended period, researchers have extensively studied and employed a multitude of traditional denoising methods to tackle the challenge of noise reduction in seismic data obtained from desert regions [14]. These techniques primarily include filtering, sparse transformations, and modal decomposition strategies. Filtering-based denoising methods work by designing specialized filters to remove noise components [15], such as high-pass filters [16], low-pass filters [17], band-pass filters [18], and F-X deconvolution filters [19]. These methods rely on differences in the frequency domain to distinguish and separate signals from noise [20]. Multi-scale methods based on wavelet transform (WT) convert seismic data into the sparse domain, utilizing the varying characteristics of signals and noise across different decomposition domains to suppress noise by setting various thresholds [21]. Similar methods include curvelet [22] and shearlet [23]. Furthermore, modal decomposition methods, such as the empirical modal decomposition (EMD) [24] and the variational modal decomposition (VMD) [25], have also been adopted to effectively handle non-stationary noise. These methods decompose seismic data into a number of intrinsic modal functions (IMFs), which are filtered and reconstructed to achieve denoising [26]. Although traditional methods perform well in certain scenarios, their limitations have become more evident as data scales and the diversity of noise types increase. For example, frequency filtering methods are prone to distortion or signal loss when faced with spectral overlap of noise and signal [27]. Multi-scale denoising methods are highly sensitive to parameter selection, frequently necessitating continuous adjustments to achieve optimal results based on the specific data conditions [28]. While modal decomposition methods are effective for handling non-stationary noise, they entail considerable computational complexity and generally require multiple iterative decompositions, rendering them less efficient for processing large-scale datasets [29]. Moreover, IMFs may simultaneously contain both valid signal and noise components [30]. If the IMFs are not properly selected, there may be partial loss of the effective signal or the presence of residual noise, which can ultimately affect the denoising result [31].

With the rapid development of deep learning, CNNs have emerged as a superior alternative to traditional denoising methods. Their ability to automatically extract features with generalization capabilities from training data enables direct application to denoising tasks, which eliminates the need for cumbersome parameter selection and tuning and thus facilitates more efficient noise suppression [32,33]. Currently, the majority of CNN denoising methods achieve high-quality denoising performance through well-designed architectural designs. For instance, feedforward denoising CNN (DnCNN) combines multiple cascaded convolutional layers, batch normalization (BN) layers, and ReLU activation functions, while also incorporating residual learning to structure the network [34]. Residual network (ResNet) builds a network architecture consisting of multiple residual blocks stacked on top of each other by introducing residual connections [35]. Furthermore, encoder-decoder architectures with skip connections, such as the residual encoder-decoder deep neural network (RED-Net) [36] and U-Net [37], modify resolution through progressive down-sampling in the encoder and up-sampling in the decoder. This enables them to achieve

effective seismic data denoising while preserving key signal features. While these network structures demonstrate notable advantages in denoising desert seismic data, they exhibit certain limitations when addressing seismic records with lower SNR. Firstly, these network structures typically rely on fixed-size convolutional kernels, making it challenging to capture both global and local features across different scales simultaneously, thereby affecting denoising precision and accuracy. Additionally, traditional CNNs gradually extract higher-level features through stacked convolutional operations, often overlooking the diversity and importance of shallow features, thereby constraining their denoising efficacy when confronted with low SNR data.

To overcome these limitations and achieve better denoising performance, a Multi-Path Guided Attention Network (MPGA-Net) with multipath structure is proposed to suppress desert noise. In this network, the primary core path employs residual strategies and dilated convolutions to extract multi-scale features. The guided enhancement path incorporates a self-guided enhancement strategy to further bolster the feature representation capabilities at each layer. The attention assisted path combines spatial and channel attention mechanisms to accurately identify and process key features, ensuring information integrity and improving precision. The experimental results show that MPGA-Net not only effectively suppresses noise but also recovers the weak reflected signals masked by surface wave, achieving superior denoising performance.

The organization of this paper is as follows. Section 1 is dedicated to introducing the research background, significance, and related research progress. Section 2 describes the network architecture and provides a detailed explanation of the MPGA-Net structure. Section 3 presents the experimental details, including the construction of the training dataset, the setting of training parameters, the configuration of the experimental environment, and the selection of comparison methods. Section 4 discusses the experimental results, validating the effectiveness of MPGA-Net in noise suppression and signal recovery through comparison experiments with synthetic record and field record. Finally, Section 5 concludes the paper.

2. **Network Architecture.**

MPGA-Net employs an innovative multi-path network architecture that integrates the primary core path, the guided enhancement path, and the attention assisted path to extract features from multiple perspectives, progressively fusing them to achieve efficient denoising. Figure 1 illustrates the architecture of MPGA-Net.

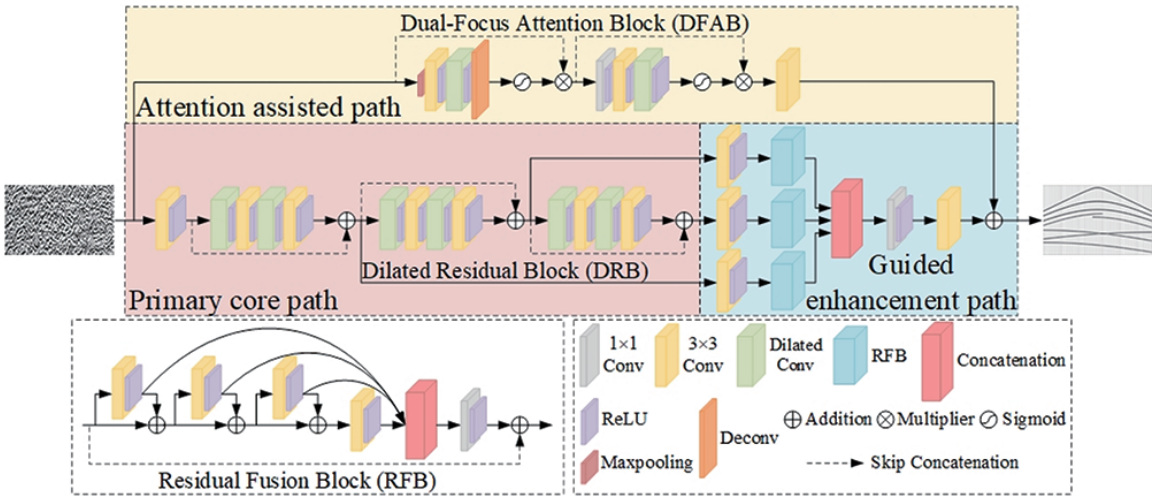

FIGURE 1. The architecture of MPGA-Net

2.1. **Primary core path.** Inspired by the residual strategy and the idea that dilated convolution contains implicit down-sampling, MPGA-Net introduces the Dilated Residual Block (DRB) in the primary core path for multi-scale feature extraction. In this path, the noisy seismic record is first preprocessed using 3×3 Conv + ReLU. Subsequently, multi-scale features, ranging from low to high levels, are extracted step by step through three stacked DRBs. Here, each DRB consists of four alternately placed dilated convolution and 3×3 convolution layer. Among these, the dilated convolution layer effectively extracts multi-scale features by expanding the receptive field, while the 3×3 convolution layer further refines the feature extraction process. The alternating application of dilated convolution and 3×3 convolution not only improves the efficiency of feature extraction but also preserves more detailed features. Additionally, the residual structure is implemented through skip connections, which not only preserve the original information but also mitigate the vanishing gradient problem.

2.2. **Guided enhancement path.** This paper proposes a new self-guided enhancement strategy designed to further enhance feature representation at all levels in the primary core path. Specifically, the output features from DRB are used as guiding information and gradually pass through a 3×3 Conv + ReLU and Residual Fusion Block (RFB) to achieve self-enhancement of the guided features. This methodology enhances both the precision and diversity of feature extraction, thereby bolstering the denoising capability. Here, RFB contains three 3×3 Conv + ReLU with residual connections and one 3×3 Conv + ReLU, which progressively extract and enhance the guided features. Based on this, the output features from the first three 3×3 Conv + ReLU are directly passed to the final stage, where they are concatenated with the output feature of the last 3×3 Conv + ReLU, forming a more enriched feature representation. Subsequently, a 1×1 Conv + ReLU is employed to reduce the number of channels, and the skip connection is introduced to facilitate the utilization of non-local features, further enhancing the denoising performance of the network. Ultimately, the features from the three guided enhancement paths are fully integrated through concatenation, which enhances the diversity of feature representation and further improves the denoising and feature extraction performance.

2.3. **Attention assisted path.** It is widely recognized that attention mechanisms significantly enhance the focus on key information while disregarding extraneous data. In MPGA-Net, the attention assisted path is introduced, utilizing a Dual-Focus Attention Block (DFAB) that combines spatial and channel attention mechanisms to enhance the network's ability to identify and process key features, thereby improving denoising accuracy. First, the noisy desert record is projected into DFAB, where the spatial attention sub-block highlights important regions spatially. Specifically, the input data undergoes max-pooling to compress its spatial dimensions. Subsequently, local spatial features are extracted using 3×3 Conv + ReLU and the receptive fields are extended by Dilated Conv + ReLU to capture higher-level semantic information. Next, the feature map is upsampled by Decovn to restore it to its original resolution. Finally, the Sigmoid function is applied to computing the spatial weights of the recovered feature maps. These weights are multiplied with the original input features to generate spatially weighted feature maps, which serve as inputs to the channel attention sub-block. In the channel attention sub-block, the main focus is on weighted fusion of feature channels to reinforce the information of important channels. First, the input features are compressed using 1×1 Conv + ReLU to reduce computational complexity and integrate information across channels. Then, the compressed features are again processed 3×3 Conv + ReLU and Dilated Conv + ReLU to further extract key features from the channel dimension. Ultimately, the channel weight maps are generated by the Sigmoid function, and these weights are multiplied with the

previous spatial feature maps to produce the final weighted channel feature maps. Finally, the output maps of DFAB are added to the fused feature maps from the guided enhancement path, further improving denoising performance.

3. **Experiment Detail.**

3.1. **Dataset preparation.**

MPGA-Net, being a supervised learning model, aims to learn and analyze data features from extensive labeled data for performing denoising on desert seismic data. Consequently, constructing the training dataset requires the inclusion of labeled data pairs, specifically composed of "clean signal-noisy signal" pairs. However, it is extremely difficult to obtain pure signals because the acquired field seismic records are inevitably contaminated by noise. In response to this challenge, this paper adopts a method that combines synthetic data with field data to construct signal dataset and noise dataset, respectively. For the signal dataset, the Ricker wavelet, the Zero-phase wavelet, and the Mixed-phase wavelet with different dominant frequencies and apparent velocities are used to generate pure signal through forward modeling. Additionally, relevant parameters are adjusted based on field seismic data to more closely approximate actual conditions. Ultimately, a total of 1000 pure records are generated, including types of signals such as curved, oblique, and intersecting axes. The specific formula is as follows:

Ricker wavelet:

$$\Psi(t) = A\left[1 - 2 \times \left(\pi f_0 (t - t_0)^2\right)\right] \times e^{-\left(\pi f_0 (t-t_0)^2\right)} \tag{1}$$

Zero-phase wavelet:

$$\Psi(t) = A\cos\left[2\pi f_0 (t - t_0)\right] \times e^{-\left(\frac{2\pi f_0 (t-t_0)}{r_1}\right)^2} \tag{2}$$

Mixed-phase wavelet:

$$\Psi(t) = A\sin\left[2\pi f_0 (t - t_0)\right] \times e^{-\left(\frac{2\pi f_\partial (t-t_0)}{r_2}\right)^2} \tag{3}$$

In Equations (1)-(3), A represents the amplitude, f_0 denotes the dominant frequency, t_0 is the start time, and r_1 and r_2 are the waveform parameters of different wavelets, respectively. Detailed parameter settings are shown in Table 1. Next, a 64×64 sliding window is used to randomly intercept 10,000 signal patches from the 100 synthetic records. Patches containing valid signals are selected and are normalized in amplitude to form a clean signal dataset. The noise dataset is constructed from passive noise records collected in the desert region, sampled at a frequency of 2,500 Hz, with a spatial sampling interval of 1 m, culminating in a total of 2,000 traces, each comprising 30,000 sampling points. These noise records are subjected to random interception using a sliding window of equivalent dimensions to the signal dataset, followed by normalization to generate a noise dataset encompassing 20,000 noise patches. Figure 2 visually elucidates the process employed in generation of both the signal and noise datasets.

Table 1. Signal dataset construction parameters

Parameters	Specifications
Seismic wavelet	Ricker, Zero-phase, Mixed-phase
Central frequency	15-40 Hz
Apparent velocity	700-3,000 m/s
Trace interval	20 m
Sample interval	2 m/s

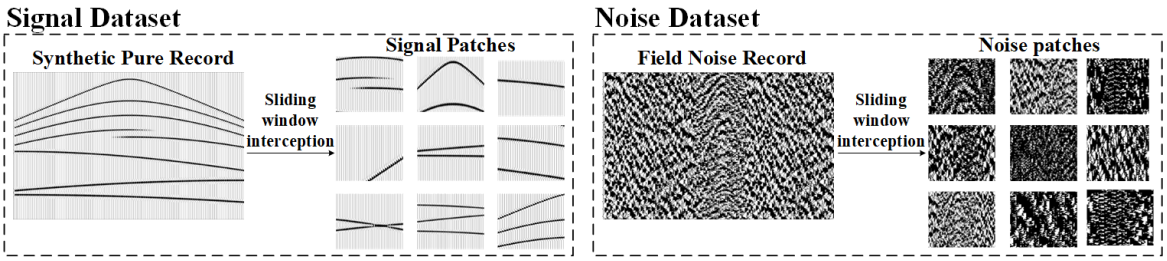

FIGURE 2. The signal dataset and noise dataset generation process

3.2. **Denoising principle and training setting.** Field seismic record is affected by environmental and equipment interference, resulting in the effective signal being obscured by various types of noise. Therefore, field seismic record can be considered as the superposition of pure signal and noise, represented by the following equation:

$$R_{noisy} = R_{pure} + R_{noise} \tag{4}$$

where R_{noisy} denotes field desert record, R_{pure} denotes pure signal, and R_{noise} denotes the noise superimposed on pure signal.

To address this issue, MPGA-Net is used to recover the effective signals from noisy record. Therefore, the denoising principle can be regarded as learning a mapping function to extract and recover the effective seismic signal, which can be specifically expressed as

$$\hat{R}_{pure} = f_\theta \left(R_{noisy} \right) \tag{5}$$

where R_{noisy} is the input noisy seismic record, $\hat{R}_{pure}$ is the clean seismic signal estimated by the network, and $f(\cdot)$ is the mapping function. The network parameters θ include weights w and biases b. By training MPGA-Net, the network learns the characteristics of pure signal from noisy record, thus enabling denoising. To ensure that the predicted signal closely approximates the effective signal, this study selects an L2 loss function to guide the training of the model, expressed as follows:

$$Loss(\theta) = \frac{1}{2N} \sum_{i=1}^{N} \left\| R_{pure,i} - \hat{R}_{pure,i} \right\|_F^2 \tag{6}$$

where N represents the batch size, $R_{pure,i}$ and $\hat{R}_{pure,i}$ denote represent the clean signal of the i-th sample and the predicted signal output by the network, respectively. $\|\cdot\|_F^2$ denotes the Frobenius norm.

Based on the denoising principle, the denoising process of MPGA-Net can be divided into three stages: dataset preparation, network training, and network testing. The dataset preparation phase is to generate the signal dataset and noise dataset for training. Signal and noise patches are then randomly selected from these datasets and combined to generate a noisy dataset with pure signals as labels. To enhance the robustness of the model, diverse noisy data are generated by increasing the variety of noise types and adjusting the SNR. During the network training stage, noisy signals from the noisy dataset are fed into MPGA-Net, where the restored signals are estimated through nonlinear mapping [38]. The error between the network output and the label data (the pure signal) is calculated and quantified using a loss function [39]. Subsequently, the gradient descent method is employed for backpropagation, optimizing the network parameters by minimizing the loss function. To accelerate the training process, the Adam optimization algorithm is employed, combined with a learning rate decay strategy to enhance training efficiency and optimization performance. The specific training parameters are provided in Table 2. After 60 epochs, the loss function stabilizes. In the network testing stage, the optimal

TABLE 2. Specific training parameters setting

Frameworks	DnCNN	U-Net	MPGA-Net
Batch size	32	32	32
Patch size	64×64	64×64	64×64
Optimizer	Adam	Adam	Adam
Learning rate range	$[10^{-4}, 10^{-6}]$	$[10^{-4}, 10^{-6}]$	$[10^{-4}, 10^{-6}]$
Epochs	60	60	60
Network layers	17	16	39
Convolutional kernel	3×3	3×3	1×1, 3×3

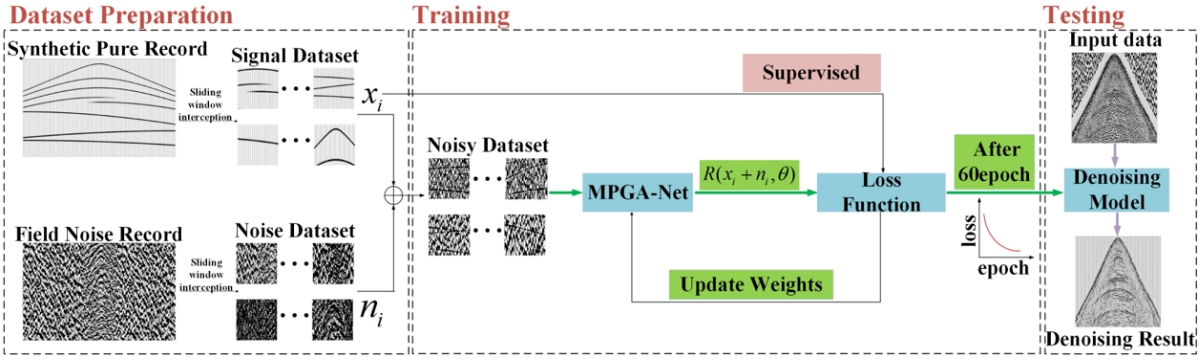

FIGURE 3. The denoising flowchart of MPGA-Net

model from the training phase is selected to process noisy seismic records [40]. Figure 3 illustrates the denoising flowchart of MPGA-Net.

3.3. **Competing methods and evaluation metrics.** To evaluate and validate the denoising performance of MPGA-Net, this study compares it with three commonly used denoising methods: EEMD, DnCNN, and U-Net. Specifically, EEMD reconstructs the signal by selecting the third and fourth modes. DnCNN is a single-scale network composed of 17 layers, whereas U-Net is a multi-scale network architecture with 16 layers. All CNN methods are trained and tested in the same experimental environment. Specifically, the software platform is MATLAB 2021b, and the hardware configuration includes an Intel i9-12900H CPU (2.50 GHz), an NVIDIA GeForce RTX 3060 laptop GPU, and 16 GB of RAM.

Based on this, all methods evaluate performance using the SNR and root mean square error (RMSE) as metrics for quantitative analysis. These metrics are applicable to seismic records under specific noise levels, to objectively evaluate the noise suppression and signal recovery effect. Here, the SNR is used to evaluate the noise suppression capability, while the RMSE measures the amplitude preservation of the signal. Usually, the ideal denoising results are shown by higher SNR and lower RMSE. The corresponding formulas are as follows:

$$SNR = 10\log_{10}\left(\frac{\sum_{i=1}^{N}\sum_{j=1}^{M}\left(R_{pure}(i,j)\right)^2}{\sum_{i=1}^{N}\sum_{j=1}^{m}\left(R_{out}(i,j)-R_{pure}(i,j)\right)^2}\right) \tag{7}$$

$$RMSE = \sqrt{\frac{1}{NM}\sum_{i=1}^{N}\sum_{j=1}^{M}\left(R_{out}(i,j)-R_{pure}(i,j)\right)^2} \tag{8}$$

where M and N denote the number of traces and time samples, respectively. Meanwhile, R_{pure} and R_{out} are the clean signals and denoised results, respectively.

4. Experiment Results.

4.1. Synthetic record processing results. In this section, we examine the denoising capability of MPGA-Net from multiple perspectives using the synthetic seismic record. Here, the synthetic noisy record is constructed by combining the synthetic pure record and the noise record. The synthetic pure record is generated by employing Ricker wavelets with dominant frequencies of 800 Hz and 600 Hz. It includes curved, fractured, and intersecting events, as shown in Figure 4(a). This helps to better simulate the complex characteristics of seismic record. The noise record is intercepted from field passive seismic record, ensuring that the noise characteristics closely resemble the actual noise interference encountered during seismic exploration, as shown in Figure 4(b). Finally, the synthetic pure record and the noise record are combined to generate the synthetic noisy record (-10 dB), as shown in Figure 4(c). Notably, strong random noise interference blurs seismic events, rendering them nearly unrecognizable.

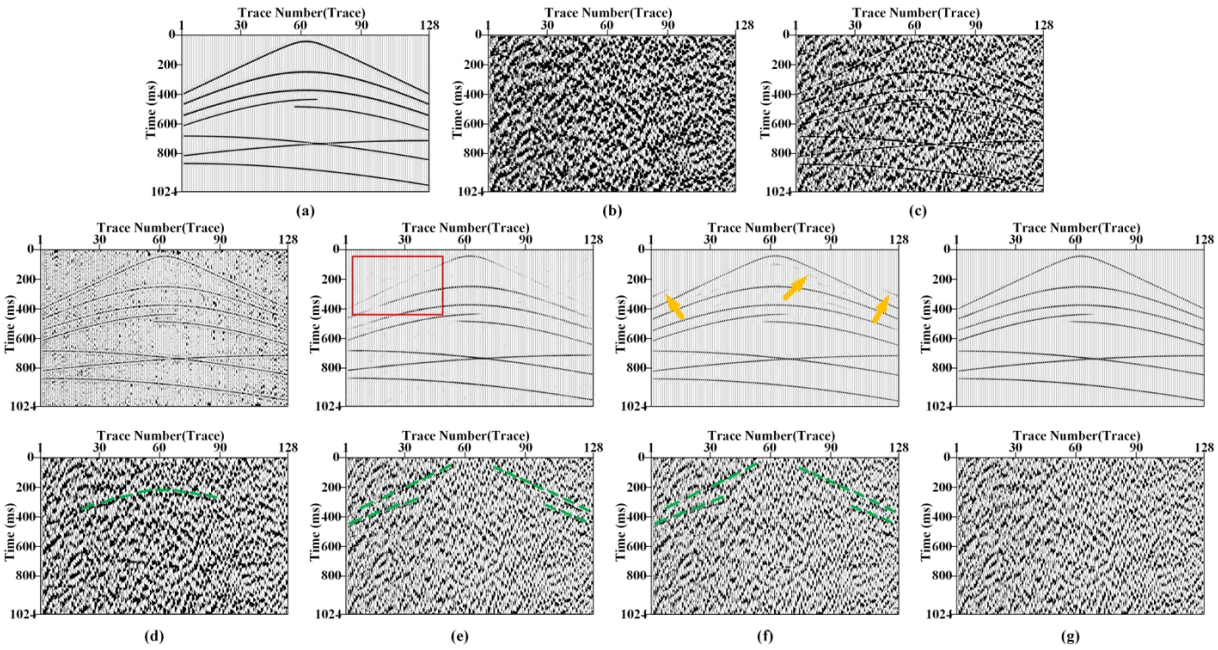

FIGURE 4. Construction of synthetic record and denoising results analysis: (a) Synthetic pure record; (b) field noise record; (c) synthetic noisy record; (d)-(g) the denoising results (top) and corresponding residual results (bottom) for EEMD, DnCNN, U-Net, and MPGA-Net, respectively

To clearly compare the noise reduction performance, we analyze the denoising results of the four methods and their residual results as shown in Figures 4(d)-4(g). It is evident that EEMD (Figure 4(d)) performs poorly in suppressing noise, with considerable random noise residue remaining and seismic events still noticeably affected by interference. Conversely, the CNN methods show superior overall denoising performance, with almost no residual noise in the denoised results. However, DnCNN (Figure 4(e)) fails to fully recover the seismic events, resulting in signal loss (as indicated by red box). U-Net (Figure 4(f)) achieves complete signal recovery, but false events remain (as indicated by yellow arrows). Comparatively, MPGA-Net (Figure 4(g)) emerges as the most effective, successfully restoring smoother and more continuous seismic events that closely resemble

the pure signal. Further comparison of the residual results reveals that EEMD, DnCNN, and U-Net exhibit varying degrees of signal leakage. In contrast, MPGA-Net has almost no signal residuals, indicating that it minimizes damage to the effective signal while still suppressing noise (as indicated by green dotted lines).

In the F-K spectrum, signal and noise typically exhibit different distribution characteristics, which forms a key basis for denoising analysis. Based on time-domain analysis results, we compare the denoised results and filtered results of MPGA-Net with those of three other methods in the F-K spectrum. The corresponding F-K spectrums are shown in Figure 5. As shown in Figure 5(a), the pure signal is clearly distributed in the F-K spectrum. However, upon the introduction of noise, significant noise interference appears in the F-K spectrum, especially in the low-frequency region where noise energy is concentrated, masking important features of the effective seismic signal. Among the four denoising methods, EEMD (Figure 5(b)) still shows a large amount of noise in the spectrum (as indicated by red box), resulting in unclear recovered signal features. DnCNN and U-Net (Figures 5(c) and 5(d)) show improved denoising performance, but signal fading (as indicated by yellow arrows) and residual noise (as indicated by red box) are still present. Furthermore, EEMD, DnCNN and U-Net exhibit different degrees of signal leakage in the filtered noise spectrum (as indicated by green dotted lines), signifying a loss of signal energy throughout the denoising process. In contrast, MPGA-Net (Figure 5(e)) not only effectively removes noise, but also preserves the detailed features of the signal.

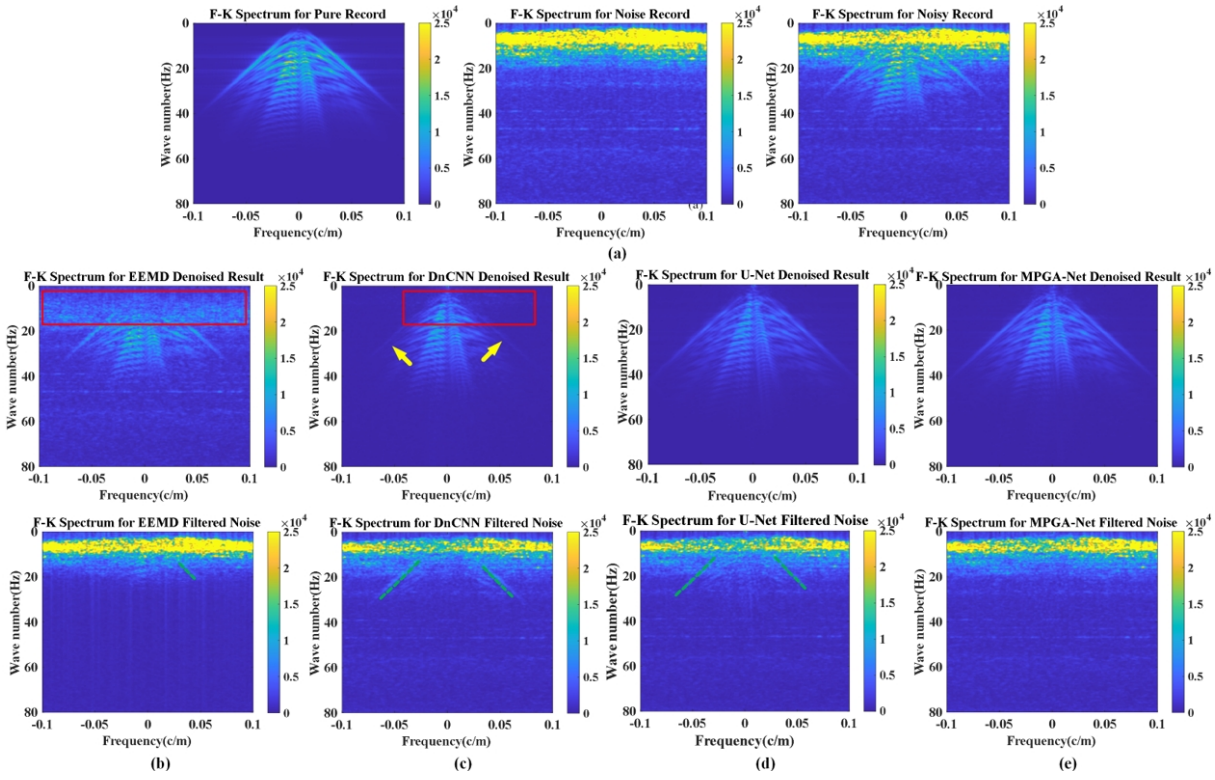

FIGURE 5. (color online) F-K spectral analysis: (a) Synthetic pure record, noise record and noisy record, respectively; (b)-(e) the denoised results (top) and corresponding filtered noise results (bottom) for EEMD, DnCNN, U-Net, and MPGA-Net, respectively

Additionally, we conduct a comparison analysis of the 115th trace record processed by the four denoising methods to further evaluate the denoising performance, as shown in Figure 6. From Figure 6(a), it is evident that the denoising result of MPGA-Net (red

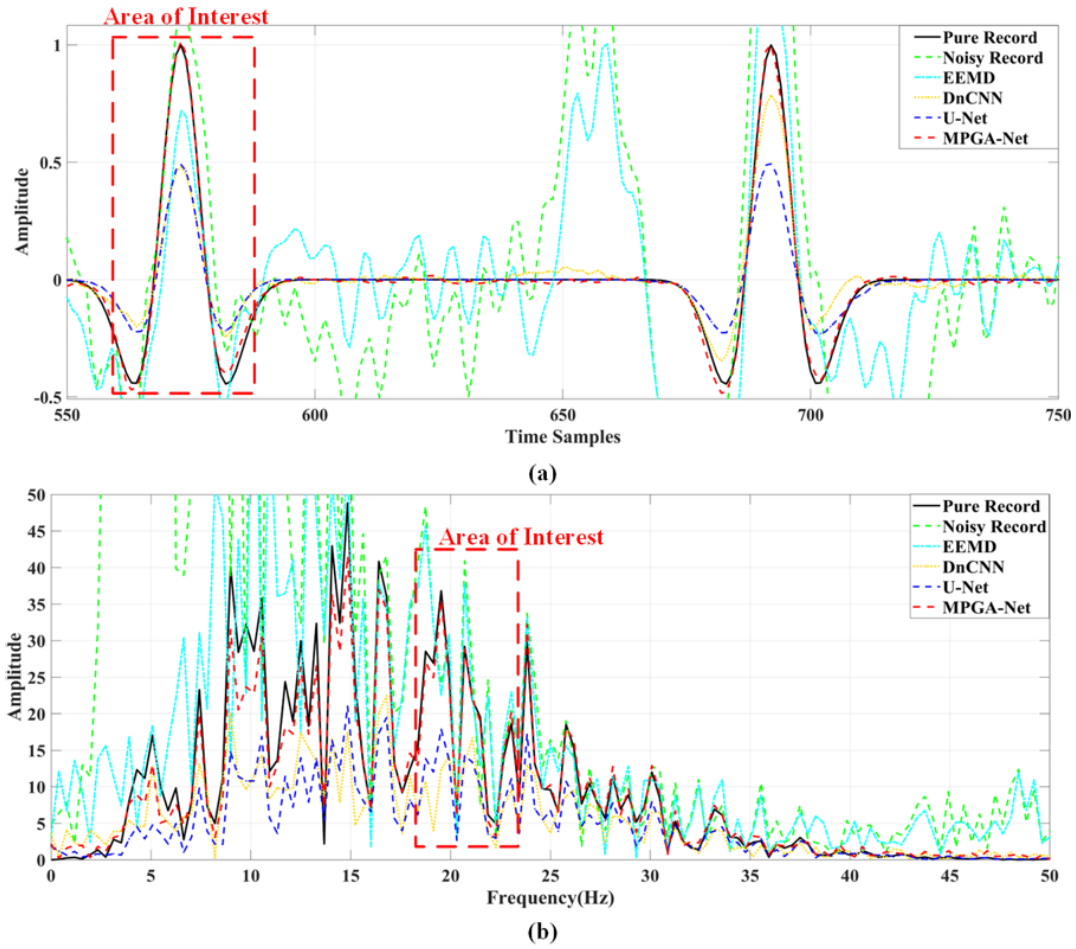

FIGURE 6. Trace record analysis: (a) Temporal plots of 115th trace record; (b) spectral distributions of 115th trace record

long dashed line) is closest to the original clean signal (black solid line), which can better preserve the key signal features. In contrast, the single trace records of EEMD (light blue short dashed line), DnCNN (yellow dotted line), and U-Net (dark blue dotted dashed line) exhibit significant waveform distortion, especially in the areas with large fluctuations (as indicated by red dotted box). In Figure 6(b), the spectrum of the signal recovered by MPGA-Net is almost identical to the original signal, while the spectral characteristics of the other three methods show significant deviations. This further demonstrates the advantages of MPGA-Net in signal recovery and noise suppression, which not only effectively removes noise, but also preserves signal integrity and detail.

Table 3 presents a comparison of the SNR and RMSE results using the four methods. It can be observed that the denoising results of MPGA-Net consistently demonstrate higher SNR and lower RMSE under the same input SNR conditions. Additionally, the data shows that MPGA-Net improves the SNR by approximately 13 dB, significantly outperforming traditional denoising methods and CNN techniques. To provide a more intuitive view of the SNR improvement effect of each method, we also calculate the local SNR of each denoised result and perform a detailed comparison analysis, as shown in Figure 7. Typically, local SNR is represented by the color intensity to reflect the strength of signal energy. From the figure, it can be seen that the energy of EEMD (Figure 7(b)) seismic events is weak, with almost no yellow areas. In contrast, the CNN methods show a more significant increase in signal energy. However, in the results of DnCNN (Figure

TABLE 3. Comparison of the SNR and RMSE results using the four methods

Original record/dB		0	−2	−4	−6	−8	−10
EEMD	SNR/dB	6.07	5.09	3.96	2.73	1.50	0.17
	RMSE	0.1184	0.1326	0.1511	0.1739	0.1985	0.2335
DnCNN	SNR/dB	9.62	9.45	9.16	8.71	8.06	6.97
	RMSE	0.0787	0.0803	0.0830	0.0873	0.0942	0.1068
U-Net	SNR/dB	9.82	9.80	9.70	9.52	9.15	8.50
	RMSE	0.0769	0.0772	0.0780	0.0797	0.0831	0.0895
MPGA-Net	SNR/dB	**13.69**	**13.47**	**13.14**	**12.68**	**12.00**	**10.80**
	RMSE	**0.0492**	**0.0505**	**0.0525**	**0.0553**	**0.0598**	**0.0687**

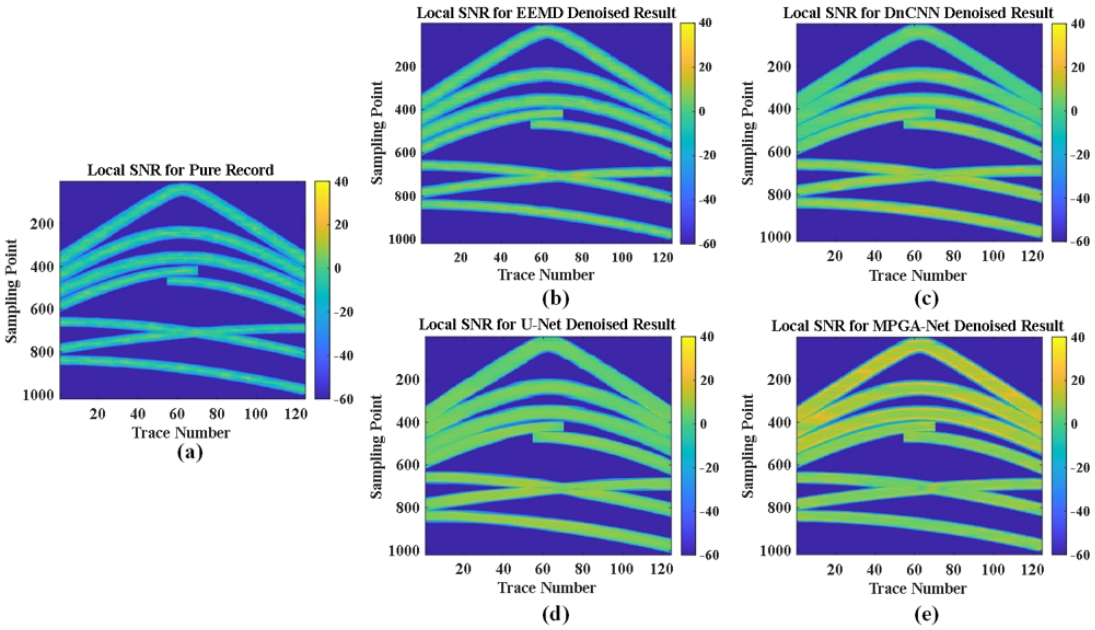

FIGURE 7. (color online) Local SNR analysis: (a) Synthetic noisy record; (b)-(e) EEMD, DnCNN, U-Net, and MPGA-Net, respectively

7(c)) and U-Net (Figure 7(d)), there are still some regions where the local SNR of the seismic events is noticeably lower than that of MPGA-Net (Figure 7(e)).

4.2. **Field data processing results.** Figure 8(a) shows 216 traces of seismic records from a common shot point acquired in desert region, with each containing 2,500 samples and a sampling interval of 4 ms. The record is heavily contaminated by random noise, significantly reducing the clarity of seismic events. Additionally, surface waves further disrupt event continuity, leading to the distortion of seismic signals. In this study, the training model for synthetic record validation is selected to process the field seismic record in Figure 8(a), with the results shown in Figures 8(b)-8(e). The results indicate that although EEMD (Figure 8(b)) suppresses some noise, significant residual random noise and surface wave interference remain, which obscure the effective events and make accurate identification challenging. In contrast, CNN denoising models perform well in noise suppression, significantly enhancing the background clarity of the processed seismic record. However, DnCNN (Figure 8(c)) and U-Net (Figure 8(d)) show poor performance in signal recovery. For example, there is almost no recovery of shallow seismic events (Area 1), and the recovery of seismic events disturbed by surface waves still exhibits breaks and discontinuities (Area 2). In contrast, the MPGA-Net (Figure 8(e)) method proposed in

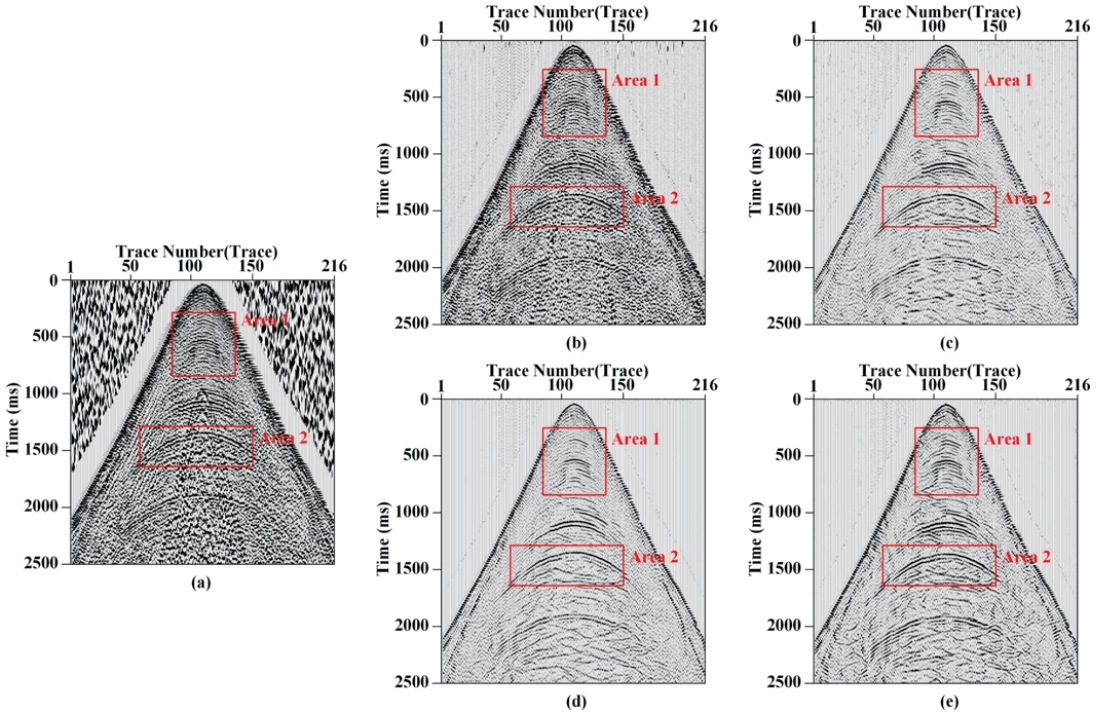

FIGURE 8. Field desert record processing results analysis: (a) Field desert record; (b)-(e) the denoising results for EEMD, DnCNN, U-Net, and MPGA-Net, respectively

this paper is effective in signal recovery, which not only performs well in the recovery of shallow reflection information, but also recovers the seismic events interfered by the surface wave better, thereby greatly improving signal continuity.

To gain a deeper understanding of the continuity of the restored signals, we conduct a detailed analysis of Areas 1 and 2 in Figure 8, with the results shown in Figures 9(a)-9(e) and 10(a)-10(e). Area 1 (Figure 9(a)) is heavily contaminated by random noise, completely obscuring the shallow information, while Area 2 (Figure 10(a)) is affected not only by random noise but also by significant surface wave interference, making the recovery of the seismic events more challenging. In Figure 9, the EEMD (Figure 9(b)) shows limited effectiveness in suppressing random noise, leaving the shallow information buried. Although DnCNN (Figure 9(c)) and U-Net (Figure 9(d)) manage to suppress random noise to some extent, the seismic events they restore lack clarity and continuity. In contrast, MPGA-Net (Figure 9(e)) demonstrates outstanding performance in restoring the continuity of the seismic events, not only providing excellent consistency but also recovering key details that DnCNN and U-Net failed to preserve. A similar pattern is observed in the analysis of Figure 10: the seismic event recovery of EEMD (Figure 10(b)), DnCNN (Figure 10(c)), and U-Net (Figure 10(d)) remains incomplete, whereas MPGA-Net (Figure 10(e)) excels in both the completeness and detail of the restored seismic events, successfully reconstructing key information that other methods could not recover.

5. **Conclusion.** This paper addresses the issue of severe noise interference in seismic data during desert exploration by proposing the MPGA-Net for attenuating desert noise. The network employs an innovative multi-path architecture that combines a guided enhancement strategy with attention mechanisms to construct three distinct paths: a primary core path, a guided enhancement path, and an attention assisted path. These paths extract features from different dimensions and progressively fuse them to achieve effective

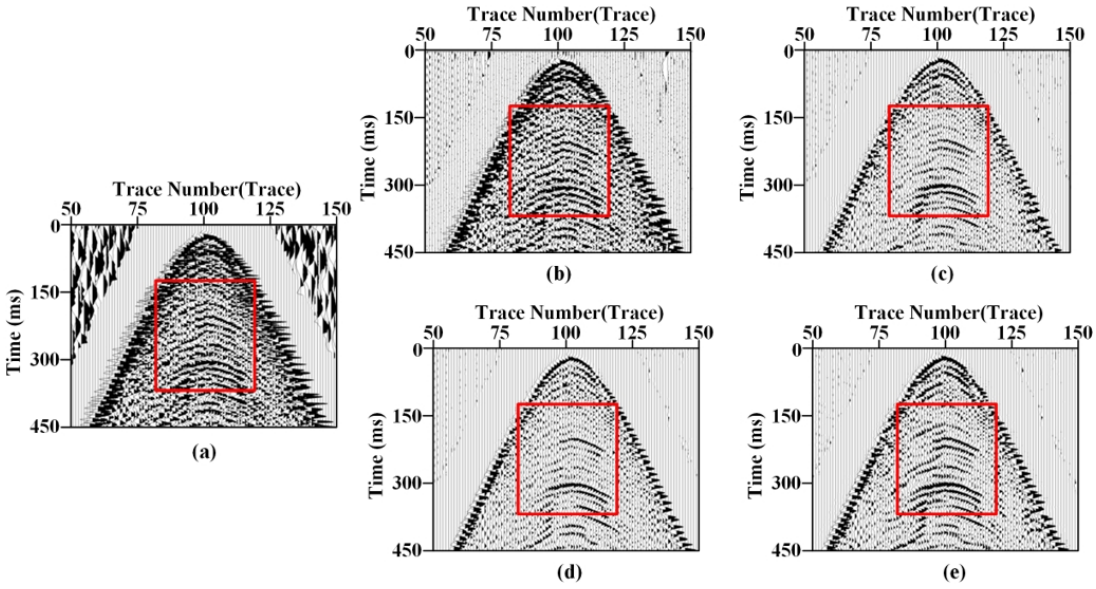

FIGURE 9. Local denoising results analysis: (a) Area 1; (b)-(e) the denoising results for EEMD, DnCNN, U-Net, and MPGA-Net, respectively

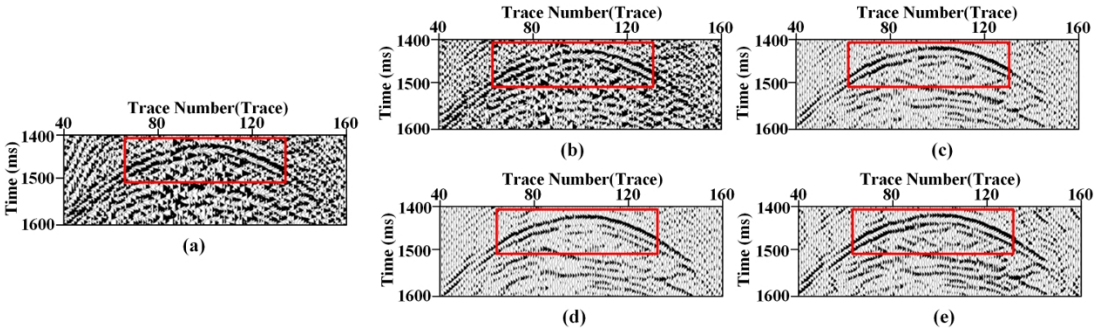

FIGURE 10. Local denoising results analysis: (a) Area 2; (b)-(e) the denoising results for EEMD, DnCNN, U-Net, and MPGA-Net, respectively

denoising. Compared to traditional denoising methods and existing CNN models, MPGA-Net demonstrates outstanding performance in noise suppression and weak signal recovery, significantly improving SNR and reducing the RMSE. Its advantages are particularly evident in handling low SNR seismic data. This study presents an effective new method for suppressing desert seismic data noise, providing a solid foundation for processing seismic data from challenging environments. Future research will further explore the applicability of MPGA-Net in addressing environmental noise in other types of seismic data, and aim to enhance denoising efficiency and performance in a broader range of seismic exploration scenarios by combining existing denoising methods with other deep learning techniques.

REFERENCES

[1] H. Wang, J. Lin, Y. Li, X. Dong, X. Tong and S. Lu, Self-supervised pretraining transformer for seismic data denoising, *IEEE Transactions on Geoscience and Remote Sensing*, vol.62, Article no.5907525, 2024.

[2] Z. Gan and X. Sun, A blended wavefield separation method for seismic exploration based on improved GoogLeNet, *PloS One*, vol.19, no.6, DOI: 10.1371/journal.pone.0304207, 2024.

[3] M. Zhang, J. Li, Y. X. Zhao, Y. Li and N. Wu, Fine-amplitude structure localization using correlation coefficients between DAS VSP data and surface seismic data at the same interface, *IEEE Geoscience and Remote Sensing Letters*, vol.21, Article no.7504905, 2024.

[4] Y. Ma, X. Cai, L. Yun, Z. Li, H. Li, S. Deng and P. Zhao, Practice and theoretical and technical progress in exploration and development of Shunbei ultra-deep carbonate oil and gas field, Tarim Basin, NW China, *Petroleum Exploration and Development*, vol.49, no.1, DOI: 10.1016/S1876-3804(22)60001-6, 2022.

[5] X. Dong, T. Zhong, H. Wang, N. Wu, Y. Li and B. Yang, The denoising of desert seismic data acquired from Tarim basin based on convolutional adversarial denoising network, *Chinese Journal of Geophysics*, vol.65, no.7, pp.2661-2672, 2022.

[6] X. Dong, H. Wang, T. Zhong and Y. Li, Desert mixed seismic noise suppression by using multiple forward models and a supervised deep-learning method, *Exploration Geophysics*, vol.52, no.4, pp.431-445, 2020.

[7] G. Li, Y. Li and B. Yang, Seismic exploration random noise on land: Modeling and application to noise suppression, *IEEE Transactions on Geoscience and Remote Sensing*, vol.55, no.8, pp.4668-4681, 2017.

[8] H. Yao, H. Ma, Y. Li and Q. Feng, DnResNeXt network for desert seismic data denoising, *IEEE Geoscience and Remote Sensing Letters*, vol.19, Article no.7501105, 2020.

[9] H. Ma, Y. Sun, N. Wu and Y. Li, Relative attributes-based generative adversarial network for desert seismic noise suppression, *IEEE Geoscience and Remote Sensing Letters*, vol.19, Article no.8023005, 2021.

[10] Y. Zhao, Y. Li and B. Yang, Low-frequency desert noise intelligent suppression in seismic data based on multiscale geometric analysis convolutional neural network, *IEEE Transactions on Geoscience and Remote Sensing*, vol.58, no.1, pp.650-665, 2020.

[11] D. Liu, H. Zhang, X. Wang, W. Chen, Z. Shi and Z. Zhao, Separation of seismic multiple reflection-refraction based on morphological component analysis with high-resolution linear Radon transform, *Geophysics*, vol.87, no.4, pp.367-379, 2022.

[12] Z. Fang, H. Lin and X. Xu, Mask-guided model for seismic data denoising, *IEEE Geoscience and Remote Sensing Letters*, vol.19, Article no.8026705, 2022.

[13] H. Ma, Y. Wang, Y. Li and Y. Zhao, Desert seismic low-frequency noise attenuation using low-rank decomposition-based denoising convolutional neural network, *IEEE Transactions on Geoscience and Remote Sensing*, vol.60, Article no.5900809, 2022.

[14] H. Ma, J. Yan and Y. Li, Low-frequency noise suppression of desert seismic data based on variational mode decomposition and low-rank component extraction, *IEEE Geoscience and Remote Sensing Letters*, vol.17, no.2, pp.337-341, 2020.

[15] C. Liu and L. Zhang, A novel denoising algorithm based on wavelet and non-local moment mean filtering, *Electronics*, vol.12, no.6, DOI: 10.3390/electronics12061461, 2023.

[16] O. Susladkar, G. Deshmukh, S. Nag, A. Mantravadi, D. Makwana, S. Ravichandran, R. S. C. Teja and G. H. Chavha, ClarifyNet: A high-pass and low-pass filtering based CNN for single image dehazing, *Journal of Systems Architecture*, vol.132, DOI: 10.1016/j.sysarc.2022.102736, 2022.

[17] I. Petras, Novel low-pass two-dimensional Mittag-Leffler filter and its application in image processing, *Fractal and Fractional*, vol.7, no.12, DOI: 10.3390/fractalfract7120881, 2023.

[18] H. T. Ma, Z. B. Qian, Y. Li, H. B. Lin, D. Shao and B. J. Yang, Noise reduction for desert seismic data using spectral kurtosis adaptive bandpass filter, *Acta Geophysical*, vol.67, no.1, pp.123-131, 2019.

[19] N. Gulunay, Signal leakage in f-x deconvolution algorithms, *Geophysics*, vol.82, no.5, pp.31-45, 2017.

[20] W. Huang, R. Wang, S. Wang, L. Cao, B. Yu and G. Shang, f-xy domain morphological filtering for three-dimensional seismic erratic noise suppression, *Geophysical Journal International*, vol.216, no.1, pp.81-102, 2019.

[21] B. Enescu, K. Ito and Z. R. Struzik, Wavelet-based multiscale resolution analysis of real and simulated time-series of earthquakes, *Geophysical Journal International*, vol.164, no.1, pp.63-74, 2006.

[22] B. Boustani, A. Javaherian, M. Nabi-Bidhendi, S. Torabi and H. R. Amindavar, Mapping channel edges in seismic data using curvelet transform and morphological filter, *Journal of Applied Geophysics*, vol.160, pp.57-68, 2019.

[23] C. Zhang and M. van der Baan, Strong random noise attenuation by shearlet transform and time-frequency peak filtering, *Geophysics*, vol.84, no.6, pp.319-331, 2019.

[24] J. Tian, Z. Tian, M. Zhang, Q. Meng, A. Zhang, C. Liu and L. Jia, A novel identification method of microseismic events based on empirical mode decomposition and artificial neural network features, *Journal of Applied Geophysics*, vol.222, DOI: 10.1016/j.jappgeo.2024.105329, 2024.

[25] Q. Ran, C. Tang, S. Han, H. Liang, Y.-J. Xue and K. Chen, Seismic noise attenuation using variational mode decomposition and the Schroedinger equation, *IEEE Transactions on Geoscience and Remote Sensing*, vol.62, Article no.4503712, 2024.

[26] T. P. Banjade, C. Zhou, H. Chen, H. Li and J. Deng, Enhancing seismic data by edge-preserving geometrical mode decomposition, *Digital Signal Processing*, vol.148, DOI: 10.1016/j.dsp.2024.104442, 2024.

[27] P. Yu, Y. Li, H. Lin and N. Wu, Seismic random noise removal by delay-compensation time-frequency peak filtering, *Journal of Geophysics and Engineering*, vol.14, no.3, pp.691-697, 2017.

[28] J. Mendel, White-noise estimators for seismic data processing in oil exploration, *IEEE Transactions on Automatic Control*, vol.22, no.5, pp.694-706, 1977.

[29] W. Huang, X. Zhu, Y. Jin and X. Shen, Nonstationary modelling of significant wave height using time series decomposition method, *Ocean Engineering*, vol.310, DOI: 10.1016/j.oceaneng.2024.118731, 2024.

[30] T. Li, R. Hou, K. Zheng, L. Li and B. Liu, A novel method of pure output modal identification based on multivariate variational mode decomposition, *Structural Control and Health Monitoring*, vol.2024, no.1, DOI: 10.1155/2024/5549641, 2024.

[31] T. Zhong, H. Chen, S. Dong and J. Li, DAS-VSP noise elimination based on the dilated pyramid attention network, *International Journal of Innovative Computing, Information and Control*, vol.19, no.5, pp.1361-1375, 2023.

[32] A. I. Hadiana, R. M. Sukma and E. K. Putra, Advanced earthquake magnitude prediction using regression and convolutional recurrent neural networks, *Jurnal Rekayasa Sistem dan Teknologi Informasi*, vol.8, no.4, pp.571-579, 2024.

[33] X. Dong, T. Zhong and Y. Li, New suppression technology for low-frequency noise in desert region: The improved robust principal component analysis based on prediction of neural network, *IEEE Transactions on Geoscience and Remote Sensing*, vol.58, no.7, pp.4680-4690, 2020.

[34] H. Fan, D. Wang, Y. Zhang, W. Wang and T. Li, Suppression of seismic random noise by deep learning combined with stationary wavelet packet transform, *Applied Geophysics*, vol.21, pp.740-751, 2024.

[35] J. Cai, L. Wang, J. Zheng, Z. Duan, L. Li and N. Chen, Denoising method for seismic co-band noise based on a U-Net network combined with a residual dense block, *Applied Sciences-Basel*, vol.90, no.3, pp.1-17, 2023.

[36] H. Ma, H. Yao, Y. Li and H. Wang, Deep residual encoder-decoder networks for desert seismic noise suppression, *IEEE Geoscience and Remote Sensing Letters*, vol.17, no.3, pp.529-533, 2020.

[37] J. Cai, L. Wang, J. Zheng, Z. Duan, F. Yan and Y. Shi, Research on U-Net seismic signal denoising combined with residual dense blocks, *Measurement Science and Technology*, vol.35, no.5, DOI: 10.1088/1361-6501/ad1fd1, 2024.

[38] T. Zhong, H. Yu, W. Wang and S. Dong, Noise suppression for DAS records using the double-scale double-path attention network, *International Journal of Innovative Computing, Information and Control*, vol.20, no.3, pp.911-928, 2024.

[39] D. T. Long, Efficient CNN model based on combining residual network and dense-connected network architectures for facial expression recognition, *International Journal of Innovative Computing, Information and Control*, vol.19, no.5, pp.1661-1678, 2023.

[40] Z. Lv, Y. Geng, H. Hou, T. Lin, X. Dai and Y. Hou, BM3D with bi-hard thresholding for image denoising in high-level noise situations, *International Journal of Innovative Computing, Information and Control*, vol.19, no.4, pp.1103-1116, 2023.

Author Biography

Tie Zhong received the B.S., M.S., and Ph.D. degrees in Communication Engineering from Jilin University, Jilin, Jilin, China, in 2006, 2008 and 2016, respectively. He is currently an Associate Professor in the Department of Communication Engineering, School of Electrical Engineering, Northeast Electric Power University, Jilin, Jilin, China. His research interests include modern signal processing techniques, weak signal process theory, and intelligent information processing.

Yaling Song received the B.S. degree in Communication Engineering from Northeast Electric Power University, Jilin, Jilin, China, in 2021. She is pursuing the M.S. degree in Information and Communication Engineering, Northeast Electric Power University. Her research interests include digital signal processing and seismic data denoising.